Journal of Molecular Catalysis A: Chemical 394 (2014) 217–223

Contents lists available at ScienceDirect

Journal of Molecular Catalysis A: Chemical

journal homepage: www.elsevier.com/locate/molcata

Wilkinson-type hydrogenation catalysts immobilized on zirconium phosphate nanoplatelets

Rita Silbernagel, Agustín Díaz, Eric Steffensmeier, Abraham Clearfield*, Janet Blümel*

Texas A&M University, Department of Chemistry, P.O. Box 30012, College Station, TX 77842-3012, USA

ARTICLE INFO

Article history:
Received 25 February 2014
Accepted 2 July 2014
Available online 17 July 2014

Keywords:
Immobilized catalysts
Zirconium phosphate
Wilkinson's catalyst
Olefin hydrogenation
Rhodium nanoparticles

ABSTRACT

Immobilized catalysts can be obtained by using a linker to bind a homogeneous catalyst to a solid support. Ideally, immobilized catalysts combine the advantages of homogeneous and heterogeneous catalysts. Porous supports such as silica result in optimal recyclability, however, the catalytic reactions are slowed down by pore diffusion. Here, non-porous zirconium phosphate nanoplatelets (ZrP) are used as support material to bridge the gap between homogeneous and immobilized catalysts. ZrP nanoplatelets provide sufficient outside surface area, while still being easily separable from the reaction mixtures. First, a phosphine linker containing an ethoxysilyl group, $(EtO)_3Si(CH_2)_3PPh_2$ (**1**), is reacted with ZrP to give the phosphine-modified **1i**. Addition of Wilkinson's catalyst $ClRh(PPh_3)_3$ to **1i** gives, via ligand exchange, the immobilized catalyst **1i–Rh**. In the absence of pore diffusion the catalytic hydrogenation of 1-dodecene using **1i–Rh** proceeds with unprecedented speed and the catalyst can be recovered and recycled 15 times. In the course of the catalytic reaction the mononuclear species forms catalytically active Rh nanoparticles on the surface. Finally it is demonstrated that $ClRh(PPh_3)_3$ can be bound to ZrP directly without linker. However, the catalytic activity of the resulting material ZrP–Rh does not quite match the favorable characteristics of **1i–Rh**.

1. Introduction

Immobilized catalysts combine in principle the advantages of homogeneous and heterogeneous catalysts and therefore they are of growing importance in academia and industry [1]. The most successful approach to obtain immobilized catalysts these days involves binding a homogeneous catalyst to a solid support with a linker. The linkers are typically bifunctional phosphines incorporating ethoxysilane groups for anchoring on oxide supports such as silica [2] or alumina [3]. The success of the immobilized catalysts is dependent on the linker type. Therefore, over the years we have explored mono- and bidentate chelate phosphine linkers for immobilized Ni [4], Rh [5], and Sonogashira Pd/Cu [6] catalyst systems. Most recently, new triphosphine linkers with long alkyl chains [7] and rigid scaffold linkers [5d,8] have led to robust immobilized olefin hydrogenation catalysts with unprecedented lifetimes. However, as a first step to test a new catalytic system, the classic and easily obtainable linker $(EtO)_3Si(CH_2)_3PPh_2$ (**1**) is still a good choice because of the ample already existing data base for comparison [5].

Most of these data available refer to olefin hydrogenation [5,9], which is of utmost importance for academia and industry. Additionally, only few reactions in transition-metal catalysis have enjoyed a more detailed investigation than hydrogenation both in solution and on surfaces [5,9]. Therefore, in this contribution we will focus on the hydrogenation of 1-dodecene as the catalytic test reaction.

Especially for industrial applications where reactor sizes and prices prohibit large amounts of bulk, porous support materials are sought because they provide a large specific surface area and therefore a maximal number of binding sites for the catalysts and consequently high loading. The popular mesoporous silica with average pore diameters of 40–200 Å is also used most often in our work [e.g. 1a,2c,d,3–8]. However, since the immobilized catalysts reside on the inner surface of the pores, the disadvantage of porous supports in general is that the necessary reaction time is prolonged because the substrates and products have to diffuse into and out of the pores. This effect is large and might increase reaction times substantially. For example, when silica with a pore diameter of 150 Å is used instead of the one with 40 Å, the hydrogenation of dodecene with an immobilized Rh catalyst takes only 30 h instead of 120 h under otherwise identical reaction conditions [7].

Therefore, an ideal support for bridging the gap between homogeneous and immobilized catalysts should provide a large external surface area which renders the tethered catalysts easily accessible

* Corresponding authors. Tel.: +1 979 845 7749; fax: +1 979 845 5629.
E-mail addresses: bluemel@tamu.edu, bluemel@mail.chem.tamu.edu (J. Blümel).

http://dx.doi.org/10.1016/j.molcata.2014.07.005
1381-1169/

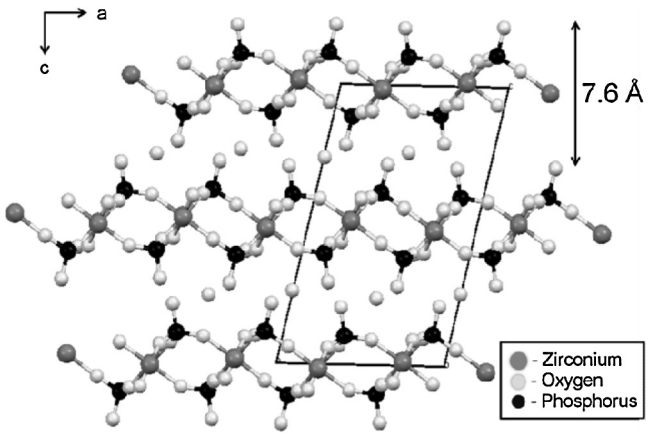

Fig. 1. α-ZrP viewed down the *b*-axis showing the interlayer spacing and intercalated water molecules. Hydrogen atoms have been omitted for clarity.

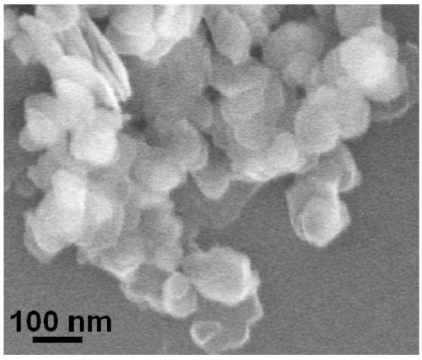

Fig. 2. SEM image of zirconium phosphate (ZrP) nanoplatelets.

to substrates without necessitating the diffusion into pores. Unfortunately, our experiments with non-porous silica (aerosil) with small particle sizes have been unsuccessful, as the material cannot be handled in an inert gas stream and does not settle from suspensions. Other groups have attempted to use, for example, nanoalumina [10], graphene oxide [11], and layered phosphonate-modified materials [12] as supports. An interesting recent approach employed a zirconium phosphate/silica system [13].

In this contribution instead of porous oxides a layered zirconium phosphate (α-ZrP, in the following: ZrP) material that has been first described by one of us [14] will be used as the support for immobilized catalysts. This material can be synthesized in a straightforward and reproducible manner [15]. Its composition has been determined as $Zr(HPO_4)_2 \cdot H_2O$ [16,17], and the crystal structure has been elucidated as monoclinic space group $P2_1/n$ [15]. The layered nature of ZrP is illustrated in Fig. 1 [16]. Each Zr atom is bonded octahedrally to six different phosphate groups, while three of the O atoms of the phosphate groups are bonded to three different Zr atoms. The fourth O atom of each phosphate group is part of a surface OH group that extends into the interlayer region. The OH proton is acidic and can be used for surface modification, e.g. with chloro- or ethoxysilanes, epoxides, or isocyanates, or for ion exchange [17,18]. X-ray powder diffraction (XRPD) reveals that the interlayer spacing is 7.6 Å [14,15].

In a first step Wilkinson-type rhodium complexes [5] will be tethered to this ZrP support via the bifunctional phosphine $(EtO)_3Si(CH_2)_3PPh_2$ (**1**). Their catalytic activity will be studied with respect to the hydrogenation of dodecene. In this way we seek to fill the missing link into the gap between homogeneous and immobilized catalysts. All catalytically active centers should be fully exposed to the surrounding solution and thus easily accessible. Therefore, fast reactions are expected and the results should not be blurred by pore diffusion.

Another incentive to radically change the nature of the support from silica to ZrP is that in the case of immobilized Rh catalysts on silica spherical Rh nanoparticles with very uniform and narrow size distribution form during hydrogenation [7]. Using a different and non-porous support material will clarify whether this nanoparticle formation is a universal feature when Rh catalysts are tethered by linkers with alkyl chains, or whether this only occurs on oxide supports. Another reason for testing a non-porous support is to investigate whether the size distribution and the regular shape of the nanoparticles in the case of silica were dominated by the pore structure as speculated in previous work [7]. In this case, with ZrP as the support, the potential nanoparticles should have a higher tendency to agglomerate and they might exhibit more irregular structures. Overall, it is expected that, with ZrP as the support, highly active catalysts are obtained that mimic the performance of homogeneous catalysts, while they can easily be separated from the reaction mixture and recycled many times.

With every new type of support it is mandatory to make sure that the basic requirements for immobilization regarding the compatibility of linker, support, and transition metal complex are fulfilled. Most fundamentally, the ethoxysilane group of the linker should bind covalently and irreversibly to the support. Otherwise the catalyst will be in danger of leaching during catalysis. Importantly, especially with respect to ZrP as the support with traces of phosphoric acid potentially left in the material from its synthesis, it needs to be checked whether phosphonium salt formation occurs as described in Ref. [19]. In this case the linker would no longer be able to coordinate to a transition metal center. Especially linkers with short alkyl chains might also decompose on the wrong type of support [20] or be prone to oxidation [19b,21].

With respect to the layered structure of the ZrP support it is also mandatory to check whether the linker is indeed only bound to the outside surface of the nanoplatelets, or whether it intercalates between the layers or even exfoliates them. In this unfavorable scenario diffusion of the substrate between the layers would again hinder the catalytic reaction or recovery of the material would be rendered problematic. Finally, one needs to investigate whether transition metal complexes such as Wilkinson's catalyst with its medium sensitivity decompose on the reactive ZrP surface or retain their integrity. Furthermore, it has to be checked whether Wilkinson's catalyst can be bound to the surface even without a linker while retaining its catalytic activity and recyclability.

In summary, the aim of the presented work is to follow the usual test protocol for new linker/support/catalyst systems, which incorporates the exploration of all points raised above using the bifunctional linker $(EtO)_3Si(CH_2)_3PPh_2$ (**1**) and Wilkinson's catalyst $ClRh(PPh_3)_3$. With this system it will ideally be possible to universally establish ZrP nanoplatelets as a practical non-porous alternative to the conventional mesoporous oxide supports. The olefin hydrogenation catalyst immobilized on the ZrP nanoplatelets with a bifunctional phosphine linker and without will be studied with respect to their activity and recyclability. Finally, the nature of the active species, whether they consist of immobilized homogeneous catalysts or nanoparticles, will be investigated.

2. Results and discussion

2.1. Support material

For the application as catalyst support material described here ZrP nanoplatelets in the size range of 150–400 nm have been prepared [15–17,22]. Fig. 2 shows the SEM image of a representative sample. Unfortunately, the smaller platelets exhibit tendencies to

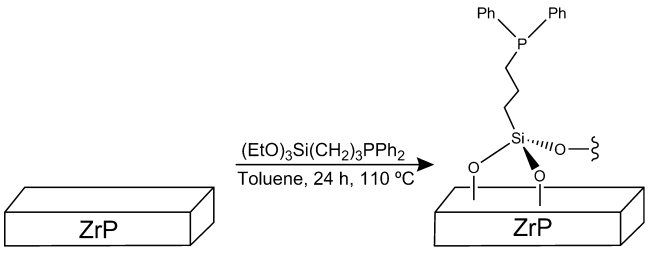

Scheme 1. Surface modification of ZrP with linker **1**.

agglomerate during the catalytic runs and thus the advantage of the easily accessible surface is lost. Other samples with small platelet sizes render their separation from the reaction mixture difficult by refusing to settle completely after the reaction, which is also obvious from the dark color of the supernatant after hydrogenation. Fortunately, the larger ZrP platelets with about 300 nm in size settle quickly after the catalytic reaction and only exhibit some agglomeration after extended periods of time. They also retain their specific surface area of 33.9 m^2/g.

2.2. Immobilization of the linker

Linker **1** has been immobilized on ZrP (Scheme 1) to form **1i** using the standard procedure applied for immobilization on oxide supports [2c,d,3–6]. After heating a mixture of **1** and ZrP in toluene to 110 °C for 24 h, the resulting material **1i** is separated from the reaction mixture by centrifugation and washed thoroughly with toluene. After drying **1i** is obtained as a white powder which is analyzed by TGA, XRPD, an electron microprobe, and solid-state NMR spectroscopy [23].

An overlay of the X-ray powder diffractogram is shown in Fig. 3. When comparing the powder diffraction pattern of pure ZrP with the pattern of **1i**, it is obvious that the peaks are broadened substantially upon immobilization. This indicates that the surface modification lowers the crystallinity of the support. Most importantly, **1** does not intercalate between the ZrP layers during the immobilization step because the interlayer spacing of 7.6 Å remains unchanged. Therefore, we conclude that all linker molecules, as well as the Rh catalyst that will be coordinated to them later, are located on the outer surface of the nanoparticles. This will lead to a fast catalytic reaction (see below) since the substrate molecules do not have to diffuse in between the support layers.

Solid-state NMR spectroscopy is the most powerful method for characterizing linkers or catalysts immobilized on silica or alumina on the molecular level [2c,d,3–8,19–23]. Since the majority of the linkers used in the community are bifunctional phosphines,

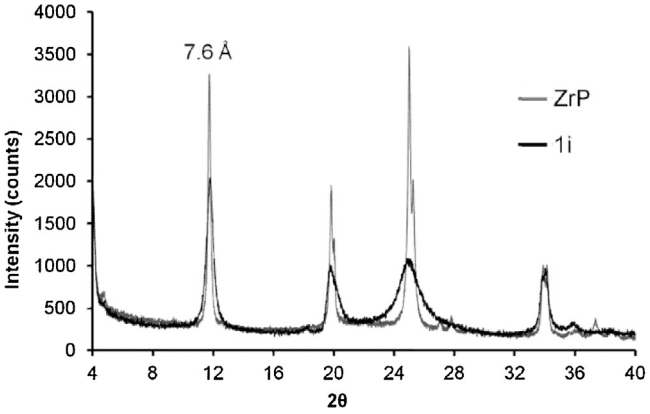

Fig. 3. XRPD overlay of ZrP sample (gray) with **1i** (black).

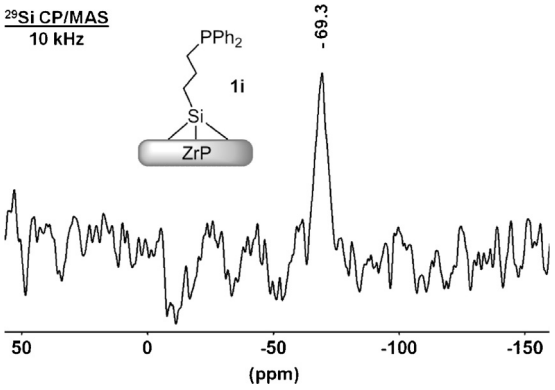

Fig. 4. ^{29}Si CP/MAS NMR spectrum of **1i** with ν_{rot} = 10 kHz.

^{31}P CP/MAS NMR of the dry materials [2c,d,3–8] or HRMAS NMR of slurries in solvents [3,6,7] are especially useful. Unfortunately, here the ^{31}P signal of the linker which is supposed to appear at ca. −18 ppm [3,19] is obscured by the huge signal of the ZrP support at about −19 ppm [16a,17d]. The signal shape and general appearance of the spectrum did not change when simple high-power decoupling was used instead of CP. However, in both cases the absence of a phosphine oxide signal which would have been expected at about 25 ppm [19b,21] indicates that the immobilized linker is very robust and **1i** can be handled in air when the material is dry. Furthermore, the absence of any phosphonium signal which would also be expected at about 25 ppm [19] proves that the phosphine is not quaternized by the acidic OH groups on the support surface. The ^{31}P CP/MAS measurement shows that careful washing of the latter is also sufficient to remove excess phosphoric acid which would result in a signal at 0 ppm.

Fortunately, the ^{29}Si CP/MAS spectrum of **1i** (Fig. 4) shows clearly one resonance even though the signal to noise ratio is not optimal because the overall content of linker on the platelets is low. Based on the chemical shift of about −69 ppm and in comparison with Ref. [24] we conclude that, in contrast to the result after binding triethoxysilanes to well-dried silica [2c,d], there is no unreacted ethoxy group left at Si. The ^{13}C solid-state NMR spectrum (Fig. 5) corroborates this assumption. Therefore, besides the alkyl substituent at Si, there must be three oxygen atoms bound to either P or H. **1i** can be bound to the ZrP support forming up to three covalent Si–O–P bridges, in analogy to forming three Si–O–Zn bridges when immobilizing ethoxysilanes on ZnO nanoparticles [25]. Although sterically not favored, this might be possible due to the nature of the surface which is not perfectly planar.

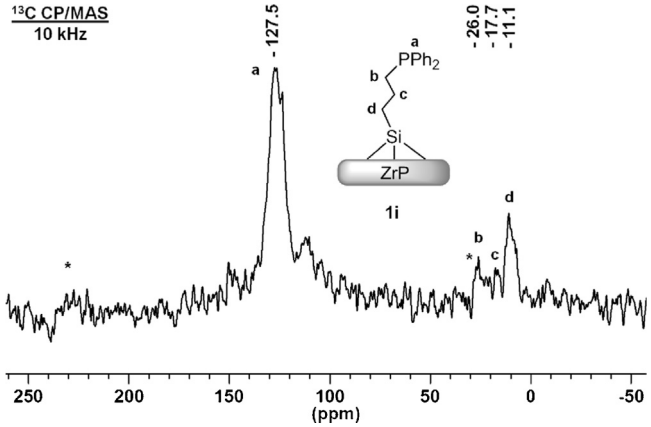

Fig. 5. ^{13}C CP/MAS NMR spectrum of **1i** with ν_{rot} = 10 kHz. Asterisks denote rotational sidebands of the aryl carbon signal.

Table 1
Microprobe atomic % data of **1i** obtained from the sample with its image shown in Fig. 6.

Sample	Atomic %			Zr:P	Zr:Si
	Si	Zr	P		
Bulk	0.4	6.7	13.8	1:1.9	17:1
Surface	0.4	0.7	1.4	1:2.2	2:1

Alternatively, one or two free or cross-linked silanol groups could be present in case of hydrolysis of the ethoxysilane groups during the immobilization step. With respect to the robust anchoring of **1** on the surface which is proven by its resistance to leaching in spite of multiple washing cycles, there has to be at least one covalent Si–O–P connection. Cross-linking of the ethoxysilanes on the support surface cannot be excluded at this point, but any growth of a gel on the surface is unlikely due to the homogeneous distribution of the linker molecules on the smooth ZrP surface as seen by microprobe analysis (see below). Furthermore, the presence of surface-detached, longer, and therefore mobile cross-linked arrays can be excluded by the absence of a ^{31}P HRMAS NMR signal of **1i**.

The ^{13}C solid-state NMR spectrum of **1i** (Fig. 5) proves the covalent binding of the linker to the ZrP support because of the characteristic residual linewidths and chemical shift anisotropies (CSA) [23b] of the signals. Although not resolved, the aryl carbon signal at about 127 ppm displays the typical large ^{13}C solid-state NMR CSA with the presence of rotational sidebands. Furthermore, in contrast to ethoxysilane–silica systems [2c,d,3], no ethoxy carbon signals are present, corroborating the above assumption regarding the binding mode. Up to three Si–O–P bonds are formed besides silanol groups due to hydrolysis (see above). Again, the poor signal to noise ratio is a consequence of the comparatively low surface area and therefore linker contents. Nevertheless the carbon signals for the alkyl chain of **1i** can be identified and assigned (Fig. 5) in analogy to cases of similar immobilized linkers [4b].

The surface coverage of **1i** with linker **1** has been obtained by determining the Si content of a sample with ICP-MS and it corresponds to 1203 linker molecules (0.678 mmol of **1**) per 100 nm^2 of surface area.

In order to determine whether the distribution of the supported linker is homogeneous on the surface of **1i**, the material is subjected to microprobe analysis. The results are given in Table 1 and Fig. 6. As the microprobe image shows, the linker distribution is even overall. The black spots are cracks in the powder pellet. The

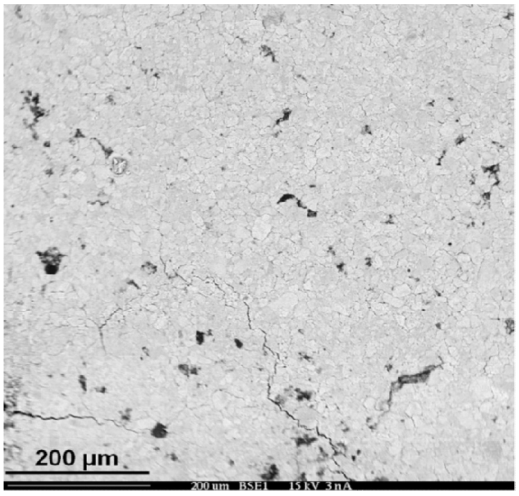

Fig. 6. Microprobe image of the surface of phosphine linker-modified ZrP nanoplatelets of **1i**.

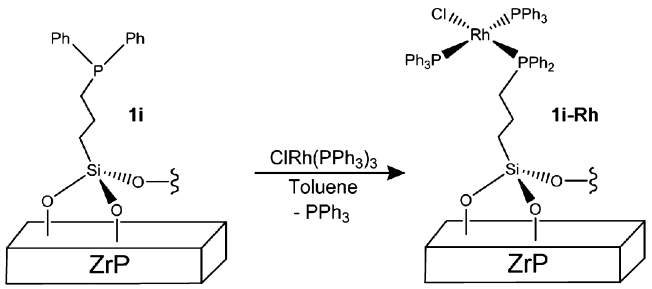

Scheme 2. Formation of the immobilized Wilkinson-type catalyst **1i**–**Rh** by ligand exchange with **1i**.

atomic ratios (Table 1) confirm that on the surface the number of Si atoms is in the same order of magnitude (0.4) as Zr (0.7), with the Zr:Si ratio being about 2:1. In the bulk, however, Zr is substantially more prevalent than Si, with a Zr:Si ratio of 17:1. This again corroborates the assumption that the silane linker **1** resides mostly on the surface of the support material, and practically does not intercalate. The microprobe analysis also indicates that the Zr:P ratio is higher in the bulk than on the surface of **1i** (Table 1), which additionally corroborates the assumption that the phosphine linker resides on the surface of the ZrP nanoplatelets and does not intercalate.

2.3. Immobilization of the catalyst

The immobilized Rh complex **1i**–**Rh** has been obtained from **1i** by ligand exchange with Wilkinson's catalyst $ClRh(PPh_3)_3$ at room temperature (Scheme 2). ^{31}P NMR shows that no free PPh_3 is found in the supernatant after washing the material with toluene. The presence and retention of the catalyst on the surface is indicated by the orange color of the support. With respect to the surface coverage of **1i** with linkers only one PPh_3 ligand is replaced at the metal center. Based on earlier ligand exchange results [5] the phosphine *trans* to the Cl ligand is most likely the one replaced by the linker. Since $ClRh(PPh_3)_3$ can also be bound to the ZrP support directly without any linker (see below), it is important to note that Wilkinson's catalyst does not intercalate between the ZrP layers. This is proven by the X-ray powder diffractogram of **1i**–**Rh** which shows the peak corresponding to the layer distance of 7.6 Å in analogy to the display in Fig. 3.

2.4. Catalysis

For testing the catalytic activity for olefin hydrogenation the procedure established previously was applied [5,7,8], using dodecene as the substrate (Scheme 3) and a hydrogenation apparatus described earlier [5c] to monitor the hydrogen consumption. With this substrate an ample data base is available [5–9] and the activity and longevity of the catalyst can be compared with the current state of the art characteristics of immobilized catalysts.

As a first test it has been established that the unmodified ZrP support does not catalyze the catalytic reaction. As expected, no H_2 uptake takes place under the standard conditions with ZrP. On the other hand, Wilkinson's catalyst in solution exhibited the usual and characteristic activity pattern [7]. In contrast, Fig. 7 shows the hydrogen uptake curves of **1i**–**Rh**. There is no induction period, and during the first run the catalyst quantitatively hydrogenates

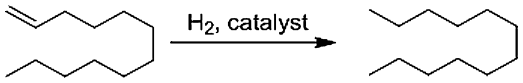

Scheme 3. Catalytic hydrogenation of 1-dodecene (pressure 1.1 atm, substrate to catalyst ratio 100 to 1, reaction temperature 25 °C, solvent toluene).

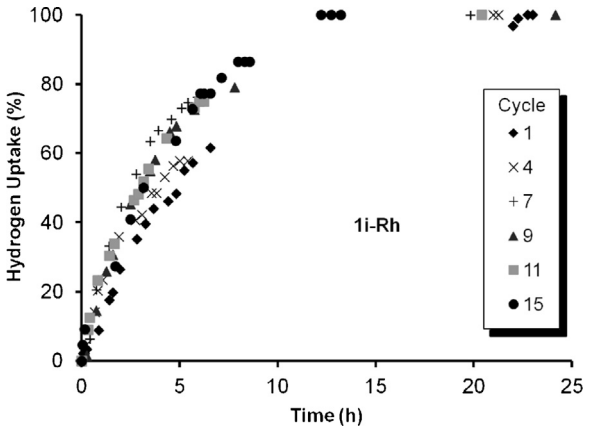

Fig. 7. Catalytic activity and recycling characteristics of **1i–Rh** for the hydrogenation of 1-dodecene.

the substrate within 23 h. When the catalyst **1i–Rh** is recycled in a batchwise manner, the activity increases somewhat and in the 15th cycle the hydrogenation is finished within 13 h. It is noteworthy to mention that the material darkens gradually and turns from beige in the first two cycles to olive green in the third cycle to black in all consecutive runs.

Although this indicates the eventual formation of nanoparticles, as described earlier for a catalyst immobilized on silica [7], the speed of the catalytic reaction is still unprecedented. Another advantage is that the material **1i–Rh** settles within a few minutes after the catalytic runs, thus facilitating its separation from the reaction mixture and recycling. For comparison, Wilkinson-type Rh complexes tethered to silica with the same ligand **1**, for example, need 32 h for this task [5a] even in the first run. Chelate complexes of Rh, bound to silica can be recycled about the same number of times, but the typical duration of one cycle with 100% substrate conversion is 35 h and an elevated reaction temperature of 60 °C is needed [5a]. Therefore, we can conclude that **1i–Rh** is the fastest immobilized hydrogenation catalyst so far, when the standard conditions (Scheme 3) are applied.

Next we further investigated the nature of the active species in the case of **1i–Rh**. The fact that the material turns black within the first three runs indicates that Rh nanoparticles might have formed during catalysis. This is also indicated by the recycling characteristics of **1i–Rh**, with its slow start, followed by high activity and finally consolidating at basically one catalytic activity curve for 13 more cycles. The analogous scenario has been found earlier with Rh catalysts immobilized by phosphine linkers with long alkyl chains [7]. In order to determine unequivocally whether nanoparticle formation takes place during catalysis with **1i–Rh**, TEM images have been recorded. Fig. 8 shows one representative image of **1i–Rh**

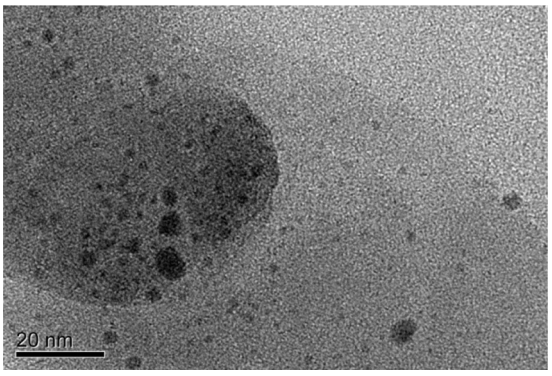

Fig. 8. TEM image of catalyst **1i–Rh** after one catalytic run.

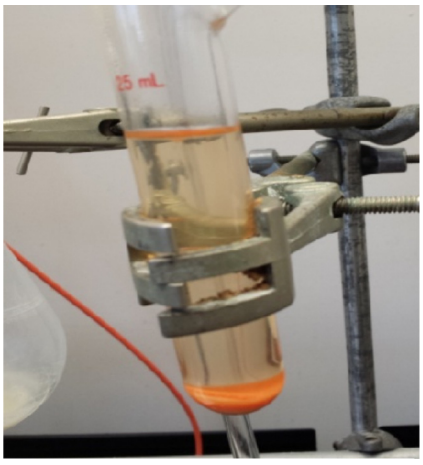

Fig. 9. The nanoparticles of ZrP–Rh settle at the bottom of the Schlenk flask after combining ZrP nanoplatelets with $ClRh(PPh_3)_3$.

after a catalytic run. Rh nanoparticles in a size range from about 1 to 8 nm are clearly visible, with those of 2–3 nm being most prevalent. Obviously, the smaller Rh nanoparticles lead to the fast catalytic reaction, as the larger particles with particle size distributions around 4–6 nm are characteristic for slower catalysts [7]. The wide variation in the nanoparticle size and the occurrence of very large irregular shaped ones indicates that the particles are not confined in pores or between the layers of the support and therefore they can grow to larger sizes. However, the great number of possible repetitive catalytic runs suggests that the nanoparticles cannot move as quickly and easily across the surface of the ZrP support to grow and thus become less active, as they can in the case of silica and in the presence of linkers with long alkyl chains [7].

Finally, it has been tested whether binding $ClRh(PPh_3)_3$ directly to the ZrP support to form **ZrP–Rh** would yield an active and recyclable catalyst. Indeed, when combining a solution of Wilkinson's catalyst with a suspension of ZrP in toluene, the initially colorless support immediately turns bright orange. Fig. 9 shows the mixture with the modified ZrP nanoplatelets in the process of settling.

Next, the activity and recycling characteristics of **ZrP–Rh** have been studied and they are represented graphically in Fig. 10. In contrast to the scenario encountered with **1i–Rh** the catalyst displays an induction period of about 2 h in the first cycle prior to assuming average activity. After a slower phase the hydrogenation is finally complete within 45 h. The time **ZrP–Rh** requires for the total substrate conversion is therefore nearly double the time needed by **1i–Rh**. Interestingly, however, the consecutive runs with **ZrP–Rh** are faster before the activity is lost again, showing the same trend observed with **1i–Rh**. In run 10 the time requirement already amounts to 90 h. While **ZrP–Rh** is therefore much less active and

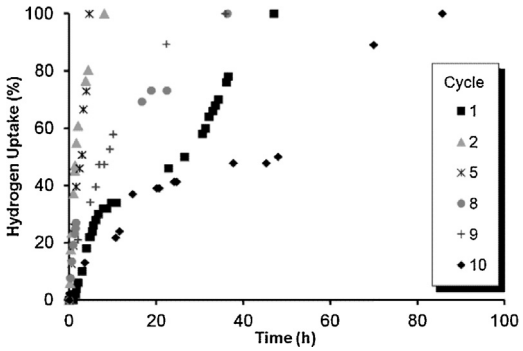

Fig. 10. Catalytic activity and recycling characteristics of ZrP-Rh for the hydrogenation of 1-dodecene.

recyclable than **1i–Rh**, it still compared favorable with immobilized Wilkinson-type Rh complexes immobilized via chelate phosphine linkers, some of which required nearly 100 h for full conversion in cycle 13 [5a].

3. Conclusion

In summary we have demonstrated that a Wilkinson-type hydrogenation catalyst can be tethered irreversibly to zirconium phosphate nanoplatelets. It has been shown that the linker is evenly "distributed" on the outside of the nanoplatelets and therefore the catalyst is dispersed homogeneously on the surface. The ligand or catalyst do not intercalate into the layers of the zirconium phosphate support. The catalyst immobilized by the phosphine linker can be easily recycled by allowing it to settle after the catalytic reaction. The most favorably sized nanoplatelets of the support do not clump during the catalytic reaction but retain their high specific surface area. Therefore, most importantly, the obtained catalyst exhibits record speed in hydrogenating the standard substrate 1-dodecene and it can be recycled 15 times in a batchwise manner without major loss of catalytic activity. Following this successful first study, which yielded the most active and recyclable immobilized hydrogenation catalyst so far, the application of chelate phosphine linkers [5a–c,6,7,20] and rigid scaffold systems [5d,8] is planned. Another point of interest is that we are not restricted to silanes as linkers as isocyanates, epoxides, phosphates and phosphonic acids also bond to the surface of α-ZrP [24]. Furthermore, the effect of varying the nanoplatelet sizes of the support material on the immobilized catalysts will be investigated.

4. Experimental

4.1. General remarks

The ^{1}H, ^{13}C, and ^{31}P NMR spectra of liquids were recorded at 499.70, 125.66, and 202.28 MHz on a 500 MHz Varian spectrometer. ^{29}Si NMR spectra of liquids were recorded at 79.37 MHz on a 400 MHz Inova spectrometer. The ^{13}C, ^{29}Si, and ^{31}P spectra were recorded with ^{1}H decoupling if not stated otherwise. The solid-state NMR spectra were measured with a Bruker Avance 400 widebore NMR spectrometer equipped with a 4 mm MAS probehead. For the CP/MAS and MAS measurements ^{1}H high-power decoupling was applied. The recycle delays were 5 s for CP/MAS, and 10 s for MAS spectra. For more measurement details, see Ref. [18b]. XRPD experiments were performed from 2° to 40° (2θ angle) as described in Ref. [15] using a Siemens D8 X-ray diffractometer system with a copper anode source (Kα1, λ = 1.5406 Å) and a filtered flat LiF secondary beam monochromator. The divergence, receiver, and detector slit widths were 2 mm, the scatter slit width was 0.6 mm. The interlayer distances were determined using Bragg's Law for the (0 0 2) diffraction plane of the diffraction pattern of α-ZrP. Transmission electron micrographs (TEM) of the samples were acquired using a JEOL 2010 transmission electron microscope at an acceleration voltage of 200 kV. Samples were prepared by drop casting a ca. 0.01% (w/w) suspension of the nanoparticles on a formvar/carbon coated copper grid from Ted Pella. All reactions were carried out using standard Schlenk techniques and a purified N_2 atmosphere, if not stated otherwise. Reagents purchased from Sigma Aldrich or VWR were used without further purification. Solvents were dried by boiling them over Na, distilled, and stored under N_2. In addition, toluene is stored under nitrogen over 3 Å molecular sieves. The ZrP nanoplatelets with sizes between 100 and 400 nm were synthesized as described in Refs. [15–17] and dried thoroughly in vacuo at RT to remove water adsorbed on the surface. The linker was synthesized following the procedure given in [19b] and the data were in accordance with the reported ones. Surface coverages were determined by ICP-MS using a Perkin-Elmer Optima 3000 dual-view ICP-MS instrument. For this purpose, 10 mg of **1i** was immersed in 10 μL of HF and diluted with 15 mL of 2% HNO_3. The atoms Zr, Si, and P were measured to determine the surface coverage of **1** on ZrP. Quantitative compositional analyses were carried out on a four spectrometer Cameca SX50 electron microprobe at an accelerating voltage of 15 kV at a beam current of 20 nA. All quantitative work employed wavelength-dispersive spectrometers (WDS). Analyses were carried out after standardization using very well characterized compounds or pure elements. Pressed powder micro pellets were prepared by pressing a few milligrams of powder between the highly polished surfaces (0.25 μm) of hardened steel dies, and transferring the pellets onto double-sided conductive carbon tape. The pellets were carbon coated before analysis to make them electrically conductive. The analyses of the pressed powder pellets were carried out with a 20 μm diameter beam while the stage was being moved 20 μm every 2 s, repeated over a ten spot traverse. This ensured representative sampling and minimized possible thermal damage to the samples.

The hydrogenation reactions were monitored using the apparatus described in Ref. [5c] by reading the consumption of hydrogen during the course of the reaction. The standard conditions listed in Scheme 3 and Refs. [5] were applied.

4.2. Immobilization of *1* on ZrP to give *1i*

400 mg (1.33 mmol) of thoroughly dried α-ZrP is placed into a Schlenk flask and 200 mL of dry, degassed toluene is added. The white opaque liquid is stirred vigorously under an argon atmosphere and 105 mg (0.267 mmol) of **1** is added via syringe. Then the reaction mixture is heated to 95 °C for 12 h while stirring vigorously. The flask is cooled and stirred for 7 more hours. Then the contents are transferred to four 50 mL centrifuge tubes and centrifuged at 5000 rpm for 15 min. The supernatant is decanted and a white solid remains. 100 mL of toluene is added to the solid for washing, and the mixture is shaken thoroughly and centrifuged. The washing process is repeated three more times. Finally, all toluene is removed and the white solid is dried under vacuum at 70 °C for 12 h. The solid material **1i** (0.3326 g, 83% with respect to ZrP) is then triturated with a mortar and pestle for 2 min and placed in a Schlenk flask for longterm storage.

4.3. Generation of *1i–Rh*

10 mg (0.01 mmol) of Wilkinson's catalyst $ClRh(PPh_3)_3$ are placed in a Schlenk flask under nitrogen and dissolved in 10 mL of toluene. Then the dark red liquid is transferred via cannula to a second Schlenk flask containing 30 mg of **1i** (corresponding to 0.077 mmol of **1**) in 10 mL of toluene. During this process the reaction mixture turns orange-brown and is stirred for 24 h at room temperature. Then the stirring is stopped and the solid **1i–Rh** settles to some degree. The supernatant appears orange/pink while the settled solid is orange/brown. The supernatant is removed via syringe and 5 mL of toluene is added. The sample is stirred again for 20 min and allowed to settle. The supernatant is removed and two more wash cycles are performed. After the third wash no more catalyst is removed from the support, as evidenced by the colorless supernatant and by ^{31}P NMR. **1i–Rh** is then suspended in 5 mL of toluene and employed for catalyzing the hydrogenation of 1-dodecene.

4.4. Generation of *ZrP–Rh*

The material **ZrP–Rh** is prepared following the procedure described for **1i**. Wilkinson's catalyst (10 mg, 0.01 mmol) is reacted

with 25 mg of ZrP at 25 °C and washed thoroughly with toluene, as outlined under **1i** above.

4.5. Hydrogenation with *1i–Rh* and *ZrP–Rh*

Immobilized catalyst **1i**–**Rh** (30 mg, containing 10 mg of Wilkinson's catalyst, corresponding to 0.010 mmol Rh) is suspended in 5 mL of toluene in a Schlenk flask. The mixture appears opaque and orange/pink in color. The flask is then attached to the hydrogenation apparatus described earlier [5c] and 1 mmol of 1-dodecene dissolved in toluene (5 mL) is added to the suspension of **1i**–**Rh** with a syringe through the stopcock. Subsequently the suspension was stirred vigorously and the hydrogen consumption was monitored. After complete substrate conversion the catalyst was allowed to settle, the supernatant was removed via syringe and the material was washed three times with 5 mL of toluene. To start the second and following cycles, fresh toluene was added and the described procedure was repeated.

For the catalysis with **ZrP**–**Rh** (25 mg, containing 10 mg of Wilkinson's catalyst, corresponding to 0.010 mmol Rh) the same procedure as outlined here for **1i**–**Rh** was applied.

Conflict of interest

The authors declare no competing financial interest.

Acknowledgments

We thank The Robert A. Welch Foundation (A-1706), NSF (CHE-0911207 and CHE-1300208), and the *APPEAL* Consortium for financial support. The authors also thankfully acknowledge the U.S. Department of Energy, Office of Nuclear Energy, Fuel Cycle Research and Development Program (AC-70059-0) through the Savannah River National Laboratory. Furthermore, we thank the Office of Basic Energy Sciences (DE-FG02-03ER15420), the National Science Foundation (DMR-0652166), and the Robert A. Welch Foundation (A-0673) for financial support. We thank B. Mosby for performing SEM measurements, Dr. V. Bakhmutov and J. Pope for recording solid-state NMR spectra, and R. Guillemette for the use of the microprobe.

References

[1] (a) P. Barbaro, F. Liguori (Eds.), Heterogenized Homogeneous Catalysts for Fine Chemicals Production, Springer, Heidelberg, 2010;
(b) J. Blümel, Coord. Chem. Rev. 252 (2008) 2410–2423;
(c) F.R. Hartley, Supported Metal Complexes, Reidel D. Publ. Co., Dordrecht, The Netherlands, 1985;
(d) D.E. DeVos, I.F.J. Vankelecom, P.A. Jacobs (Eds.), Chiral Catalyst Immobilization and Recycling, Wiley-VCH, Weinheim, 2000;
(e) G. Rothenberg, Catalysis: Concepts and Green Applications, Wiley-VCH, Weinheim, 2008.

[2] (a) E.F. Vansant, P. VanDer Voort, K.C. Vrancken, Characterization and Chemical Modification of the Silica Surface, Elsevier, Amsterdam, 1995;
(b) R.P.W. Scott, Silica Gel and Bonded Phases, John Wiley and Sons, New York, 1993;
(c) J. Blümel, J. Am. Chem. Soc. 117 (1995) 2112–2113;
(d) K.D. Behringer, J. Blümel, J. Liq. Chromatogr. 19 (1996) 2753–2765.

[3] C. Merckle, J. Blümel, Chem. Mater. 13 (2001) 3617–3623.

[4] (a) S. Reinhard, K.D. Behringer, J. Blümel, New J. Chem. 27 (2003) 776–778;
(b) S. Reinhard, P. Soba, F. Rominger, J. Blümel, Adv. Synth. Catal. 345 (2003) 589–602.

[5] (a) C. Merckle, J. Blümel, Adv. Synth. Catal. 345 (2003) 584–588;
(b) C. Merckle, J. Blümel, Top. Catal. 34 (2005) 5–15;
(c) C. Merckle, S. Haubrich, J. Blümel, J. Organomet. Chem. 627 (2001) 44–54;
(d) B. Beele, J. Guenther, M. Perera, M. Stach, T. Oeser, J. Blümel, New J. Chem. 34 (2010) 2729–2731.

[6] (a) T. Posset, J. Blümel, J. Am. Chem. Soc. 128 (2006) 8394–8395;
(b) T. Posset, J. Guenther, J. Pope, T. Oeser, J. Blümel, Chem. Commun. 47 (2011) 2059–2061.

[7] J. Guenther, J. Reibenspies, J. Blümel, Adv. Synth. Catal. 353 (2011) 443–460.

[8] Y. Yang, B. Beele, J. Blümel, J. Am. Chem. Soc. 130 (2008) 3771–3773.

[9] (a) J.G. de Vries, C.J. Elsevier (Eds.), The Handbook of Homogeneous Hydrogenation, Vols. 1–3, 1st ed., Wiley-VCH, Weinheim, 2007;
(b) G. Ertl, F. Knözinger, J. Schüth (Eds.), Handbook of Heterogeneous Catalysis, 2nd ed., Wiley-VCH, Weinheim, 2008;
(c) M. Wende, R. Meier, J.A. Gladysz, J. Am. Chem. Soc. 123 (2001) 11490 (and lit. cited therein);
(d) Adv. Synth. Catal. 345 (2003), vols. 1 + 2, Special Issue on Hydrogenation, including, e.g.: W.S. Knowles, Adv. Synth. Catal. 345 (2003) 3; R. Noyori, Adv. Synth. Catal. 345 (2003) 15; T. Imamoto, Adv. Synth. Catal. 345 (2003) 79.;
(e) D.M. Heinekey, A. Lledós, J.M. Lluch, Chem. Soc. Rev. 33 (2004) 175–182.

[10] P. Li, W. Thitsartarn, S. Kawi, Ind. Eng. Chem. Res. 48 (2009) 1824–1830.

[11] Z. Qingshan, D. Chen, Y. Li, G. Zhang, F. Zhang, X. Fan, Nanoscale 5 (2013) 882–885.

[12] (a) S. Bischoff, A. Kockritz, M. Kant, Top. Catal. 13 (2000) 327–334;
(b) J.W. Bae, S.J. Park, M.H. Woo, J.Y. Cheon, K.S. Ha, K.W. Jun, D.H. Lee, H.M. Jung, ChemCatChem 3 (2011) 1342–1347.

[13] R. Joshi, U. Chudasama, Ind. Eng. Chem. Res. 49 (2010) 2543–2547.

[14] A. Clearfield, J.A. Stynes, J. Inorg. Nucl. Chem. 26 (1964) 117–129.

[15] J.M. Troup, A. Clearfield, Inorg. Chem. 16 (1977) 3311–3314.

[16] (a) B.M. Mosby, A. Díaz, V. Bakhmutov, A. Clearfield, Appl. Mater. Interfaces 6 (2014) 585–592;
(b) C.Y. Ortiz-Avila, A. Clearfield, Inorg. Chem. 24 (1985) 1773–1778.

[17] (a) M. Casciola, D. Capitani, A. Donnadio, G. Munari, M. Pica, Inorg. Chem. 49 (2010) 3329–3336;
(b) M. Pica, A. Donnadio, E. Troni, D. Capitani, M. Casciola, Inorg. Chem. 52 (2013) 7680–7687;
(c) M. Pica, A. Donnadio, D. Capitani, R. Vivani, E. Troni, M. Casciola, Inorg. Chem. 50 (2011) 11623–11630;
(d) H. Nakayama, Phosphorus Res. Bull 23 (2009) 1–9.

[18] A.F. Mejia, A. Díaz, S. Pullela, Y.-W. Chang, M. Simonetty, C. Carpenter, J.D. Batteas, M.S. Mannan, A. Clearfield, Z. Cheng, Soft Matter 8 (2012) 10245–10253.

[19] (a) J. Sommer, Y. Yang, D. Rambow, J. Blümel, Inorg. Chem. 43 (2004) 7561–7563;
(b) J. Blümel, Inorg. Chem. 33 (1994) 5050–5056.

[20] T. Posset, F. Rominger, J. Blümel, Chem. Mater. 17 (2005) 586–595.

[21] C.R. Hilliard, N. Bhuvanesh, J.A. Gladysz, J. Blümel, Dalton Trans. 41 (2012) 1742–1754.

[22] L. Sun, W.J. Boo, H.-J. Sue, A. Clearfield, New J. Chem. 31 (2007) 39–43.

[23] (a) C.A. Fyfe, Solid-State NMR for Chemists, C.F.C. Press, Guelph, Canada, 1983;
(b) T.M. Duncan, A Compilation of Chemical Shift Anisotropies, Farragut Press, Chicago, IL, 1990;
(c) S. Reinhard, J. Blümel, Magn. Reson. Chem. 41 (2003) 406.

[24] A. Díaz, B.M. Mosby, V. Bakhmutov, A.A. Martí, J.D. Batteas, A. Clearfield, Chem. Mater. 25 (2013) 723–728.

[25] M. Wong, J. Guenther, L. Sun, J. Blümel, N. Nishimura, H.-J. Sue, Adv. Funct. Mater. 22 (2012) 3614–3624.